# PROCEEDINGS OF SPIE

SPIEDigitalLibrary.org/conference-proceedings-of-spie

# Characterizing atmospheric turbulence over Maunakea through temporal tomography

Ryan Dungee, Mark Chun

Ryan Dungee, Mark Chun, "Characterizing atmospheric turbulence over Maunakea through temporal tomography," Proc. SPIE 12185, Adaptive Optics Systems VIII, 121851P (29 August 2022); doi: 10.1117/12.2628413



Event: SPIE Astronomical Telescopes + Instrumentation, 2022, Montréal, Québec, Canada

# Characterizing atmospheric turbulence over Maunakea through temporal tomography

Ryan Dungee<sup>a</sup> and Mark Chun<sup>a</sup>

<sup>a</sup>Institute for Astronomy, University of Hawai'i, 40 North A'ohōkū Place, Hilo, HI, 96720, USA

# ABSTRACT

Early adaptive optics (AO) systems were designed with knowledge of a site's distribution of Fried parameter  $(r_0)$  and Greenwood time delay  $(\tau_0)$  values. Recent systems have leveraged additional knowledge of the distribution of turbulence with altitude. We present measurements of the atmosphere above Maunakea, Hawaii and how the temporal properties of the turbulence relate to tomographic reconstructions. We combine archival telemetry collected by 'imaka—a ground layer AO (GLAO) system on the UH88" telescope—with data from the local weather towers, weather forecasting models, and weather balloon launches, to study how frequently one can map a turbulent layer's wind vector to its altitude. Finally, we present the initial results of designing a new GLAO control system based off of these results, an approach we have named "temporal tomography."

**Keywords:** Ground Layer, Adaptive Optics, Turbulence Profiling

#### 1. INTRODUCTION

The designs of early adaptive optics (AO) systems were largely based on relatively few site characteristics. Distributions of the Fried parameters  $(r_0)$  and Greenwood time delay  $(\tau_0)$  values were sufficient to set the system requirements and understand the expected performance. However, more complex AO systems generally leverage additional knowledge of a site's turbulence characteristics, such as knowledge of the vertical distribution of turbulence strength for multi-conjugate AO (MCAO). A variety of techniques exist for studying the spatial and temporal characteristics of a site's turbulence. Approaches such as Slope Detection and Ranging<sup>1-3</sup> (SLODAR) and Fourier Wind Identification<sup>4,5</sup> (FWI) allow these measurements to be done using the data collected during regular AO operations, critical for developing a long term picture of turbulence characteristics.

In this paper we present our progress on utilizing external measurements of wind speed and direction in combination with wavefront sensor data to: 1) identify the dominant turbulent layers in the atmosphere, and 2) assign these layers an altitude based on their wind speeds and directions. In particular we consider the application of this technique to ground layer AO (GLAO), where the goal is to filter out the free atmosphere signal in the wavefront sensor measurements and thus improve the estimate of the ground layer. We call this technique "temporal tomography" since it relies on the temporal power spectra of the wavefront sensor data. Successful temporal tomography is expected to yield a number of benefits. By reducing the signal of the free atmosphere, fewer guide stars are required to obtain an accurate measure of the ground layer turbulence. This would reduce the cost of laser guide star-based systems by requiring fewer laser beacons and wavefront sensors. For natural guide star-based systems requiring fewer stars of sufficient brightness in the field will increase the sky coverage of the system. Such benefits would facilitate the wide spread adoption of GLAO.

Further author information: (Send correspondence to R.D.)

R.D.: E-mail: rdungee@hawaii.edu M.C.: E-mail: markchun@hawaii.edu

### 2. METHOD

The basic principle behind temporal tomography is that atmospheric layers with different wind vectors will have power concentrated at different temporal frequencies. In theory, any modal basis for which this is true (e.g., Zernike modes<sup>6</sup>) can be used with the concepts laid out in this section. Here, we use the complex Fourier modes of the slopes, which are simply the discrete Fourier transform (DFT) of the wavefront sensor slopes. These can be converted into the Fourier modes of the phase through multiplication with a complex-valued filter,<sup>7,8</sup> though we do not take that step here. In this basis an atmospheric layer with wind vector  $\langle v_x, v_y \rangle$  will lead to a peak in the temporal power spectrum of each of the Fourier modes, and that power will be centered on the frequency:<sup>8</sup>

$$f_t = -\frac{kv_x + lv_y}{Nd} \tag{1}$$

where k and l are the Fourier mode indices, d is the subaperture size, and N is the order of the wavefront sensor (assuming a wavefront sensor grid that is  $N \times N$  subapertures). By using the complex Fourier modes as the basis, the power spectra are not symmetric about 0 Hz, and as a result  $f_t$  can be positive or negative. Therefore, the sign of  $f_t$  provides information on how the wind vector  $\langle v_x, v_y \rangle$  projects onto the Fourier mode vector  $\langle k, l \rangle$ . In principle, an atmospheric layer will produce a peak in the power spectra of each Fourier mode and by cross-matching all of the peaks across all of the power spectra, typically by brute force,  $^{4,5}$  one can back out the number of turbulent layers in the atmosphere and their wind vectors. Combining this with knowledge of the vertical wind profile enables one to map these turbulent layers to altitudes. Such an approach will ultimately be limited by how different the wind speeds and directions are as a function of altitude, something we explore further in Sec. 3.1.

When each atmospheric layer has a unique wind vector, and thus a unique set of  $f_t$  values in each of the power spectra, one can leverage this information in the AO control loop. In particular we look at the case of using temporal tomography to produce an improved GLAO correction. In a traditional GLAO system, the estimate of the ground layer turbulence is produced by the average wavefront obtained from multiple, widely separated, guide stars. If the free atmosphere turbulence probed by each of the guide stars is uncorrelated, then it averages down and the estimate of the ground layer improves roughly as the square root of the number of guide stars. However, this means that there is some residual free atmosphere signal in the estimate of the ground layer, and this is injected into the correction applied by the system. Our aim is to improve the GLAO correction by filtering out the excess power in each mode originating from the free atmosphere prior to reconstruction. At a high level the approach is to: 1) calculate the slope Fourier modes by applying the DFT to the wavefront sensor slopes, 2) apply a recursive filter to each of these Fourier modes, and 3) apply the inverse DFT to the Fourier modes generating a set of filtered slopes that are then processed by the same means as a standard GLAO system. The recursive filters used in the second step are designed based on the temporal power spectra of that night. We used notch reject filters with bandwidths of 15 Hz centered on the free atmosphere  $f_t$  values for the simulations presented in Sec. 3.2. Optimization of the filter design is left for future work. However, for on-sky operations the  $f_t$  values for the free atmosphere are not necessarily known beforehand. Fortunately, most astronomical sites have weather towers that provide real time measurements of the ground layer wind vectors, from which we can calculate the ground layer  $f_t$  values. Since the goal is to reject any free atmosphere turbulence from our correction, we can take the simple approach of assuming all other peaks in the temporal power spectra are free atmosphere, and thus should be filtered from the slope measurements\*. This approach allows us to selectively remove the free atmosphere signal from the wavefront sensor data, resulting in a better estimate of the ground layer than averaging alone.

# 3. FEASIBILITY

# 3.1 Atmospheric Statistics

Critical to our approach is that the wind vectors are different enough to be resolved as separate peaks in the power spectra of the Fourier modes. To understand how frequently this is the case for separating the ground

<sup>\*</sup>There may also be peaks due to vibrations in the system, ignoring them here simply means the system will see and try to correct for them.

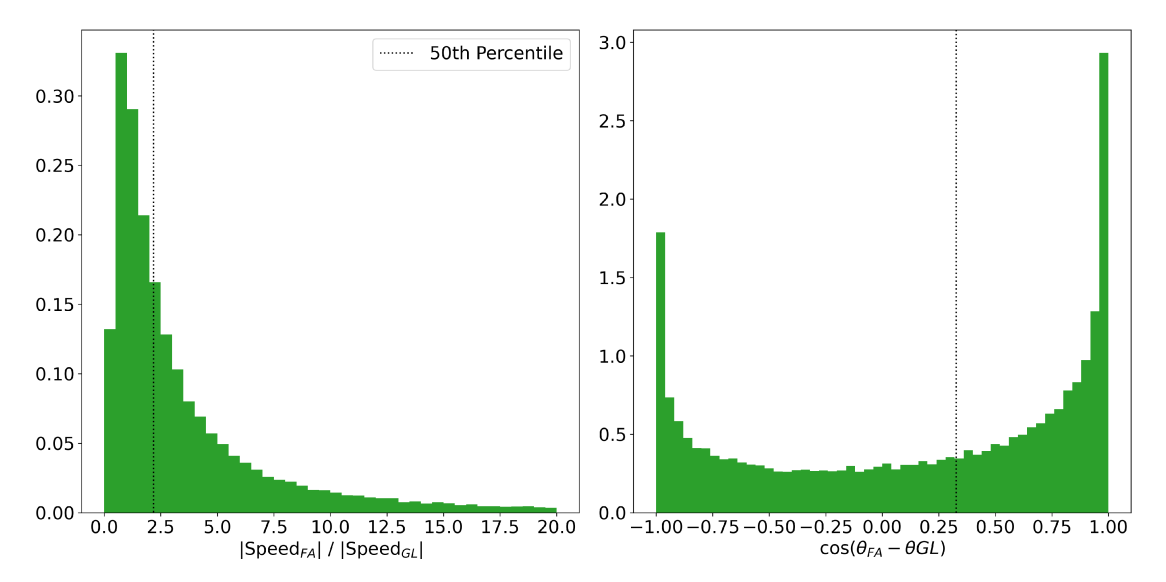


Figure 1. Left Panel: The distribution of the ratios of the free atmosphere wind speed to the ground layer wind speed. Right Panel: The distribution of the dot product of the unit vectors of the free atmosphere and ground layer wind directions. Both Panels: The full distributions of the metrics discussed in Sec. 3.1, computed for 1551 nights spanning January 1st, 2018 to July 6th, 2022. The vertical dotted line is the 50th percentile. By these two metrics the ground layer is easily separable from the free atmosphere based on wind vectors  $\sim 67\%$  of time.

layer turbulence from the free atmosphere we collected data on the vertical profiles of wind speeds and directions from the Maunakea Weather Center's data archive. For the free atmosphere wind speeds and directions we use the profiles provided by the Global Forecasting System (GFS) weather models<sup>†</sup>. The GFS models for Maunakea provide a forecasted wind speed and direction for 13 different layers in the atmosphere, at pressures ranging from 700 millibars to 100 millibars, in steps of 50. Every six hours a new forecast is produced which includes the predicted wind speed and direction for each layer at times ranging from 0 hours to 180 hours into the future. Every 12 hours the model is updated to include data collected from weather balloons launched from the Hilo International Airport, and thus the 0-hour forecasts from GFS models at 00:00 and 12:00 (UTC) accurately represent the measured vertical profile of the wind. We restrict our dataset to the nighttime profiles, giving us one profile per night, from January 1st, 2018 to July 6th, 2022. Finally, the pressure measured by the Canada France Hawaii Telescope's (CFHT) weather tower at the summit is typically close to 600 millibars, so we only consider the layers with pressures of 550 millibars or less to be free atmosphere, yielding 10 free atmosphere layers.

For the ground layer wind speeds and directions we use the Canada France Hawaii Telescope's (CFHT) weather tower<sup>‡</sup>. Because these data are reported every 5 minutes, whereas the free atmosphere values are only available once a night, we computed a nightly mean and standard deviation from the CFHT measurements to serve as representative values. The mean ground layer wind vector is calculated component-wise and the standard deviation of the speeds is calculated using the standard method applied to the measured wind speeds. The standard deviation of the directions is estimated using the Yamartino method, which properly accounts for the fact that angles are periodic. Specifically, for n measurements of the wind direction  $\theta$ :

$$\sigma_{\theta} = \arcsin(\epsilon) \left[ 1 + \left( \frac{2}{\sqrt{3}} - 1 \right) \epsilon^3 \right]$$
 (2)

where  $\epsilon = \sqrt{1 - (s_a^2 + c_a^2)}$ ,  $s_a = \frac{1}{n} \Sigma_i^n \sin \theta_i$ , and  $c_a = \frac{1}{n} \Sigma_i^n \cos \theta_i$ . We then characterized each night with three ground layer wind speeds/directions, the mean and the mean plus or minus one standard deviation.

<sup>&</sup>lt;sup>†</sup>The archival data can be found on this page of the website.

<sup>&</sup>lt;sup>‡</sup>The archival data can be found on this page of the website.

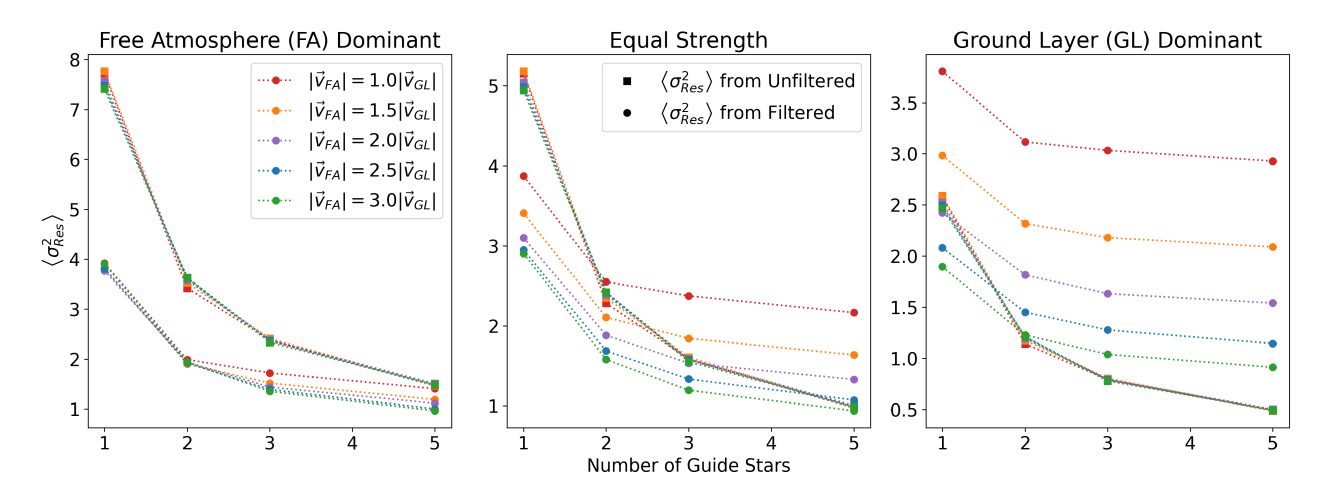


Figure 2. The mean variance of the residual wavefronts for each simulation, where the residual wavefront is the difference between an estimation of the ground layer and the ideal reconstruction of the ground layer. In each panel the color corresponds to the wind speed of the free atmosphere for that simulation, squares represent the results of the standard GLAO reconstruction and circles represent the reconstruction with filtering of the slope Fourier modes. When the atmosphere is dominated by the free atmosphere filtering allows a 2 guide star system to perform comparably to a 5 guide star system. On a ground layer dominant night the filter that was used removes some of the ground layer signal as well, resulting in a worse estimate than the standard approach.

Next, we considered two metrics for how different the ground layer wind was from the free atmosphere layers in a given night. First, we calculated the ratio of the wind speeds:  $\frac{\text{Speed}_{FA}}{\text{Speed}_{GL}}$ , since the wind speed is directly proportional to the  $f_t$ -value of the layer this value corresponds roughly to the ratio of the free atmosphere  $f_t$  to the ground layer  $f_t$ , the farther this value is from one, the better. Second, we calculated the dot product of the unit direction vectors:  $\cos(\theta_{FA} - \theta_{GL})$ . These values ranged from -1 to 1, and again the farther this value is from one, the better. Then for each night we calculated these values for every combination of 3 ground layer speed/directions and 10 free atmosphere speed/directions, giving 30 wind speed ratios and 30 wind direction dot products per night. The full distribution of each of these metrics can be seen in Fig. 1.

Ultimately, the ability to resolve two separate peaks in the power spectrum will also depend on the AO system that is being used and the characteristics of the turbulence itself. Nonetheless, these distributions provide useful, if rough, estimates for how often temporal tomography can be expected to successfully sort atmospheric layers between ground layer and free atmosphere. A best case scenario is when the ground layer and the free atmosphere layer have directions that are anti-aligned (i.e.  $\cos{(\theta_{FA} - \theta_{GL})} < 0$ ), as this means the  $f_t$  value for each layers will always have opposite signs. For all the nights in our sample, this is the case  $\sim 36\%$  of time. Of the nights where the two are roughly aligned (i.e.  $\cos{(\theta_{FA} - \theta_{GL})} > 0$ ), then they must have different speeds for temporal tomography to work. If we conservatively require the two layers to be different by a factor of two (i.e.  $\frac{\text{Speed}_{FA}}{\text{Speed}_{GL}} > 2$  or  $\frac{\text{Speed}_{FA}}{\text{Speed}_{GL}} < 0.5$ ), this covers another  $\sim 31\%$  of all nights. This means that for  $\sim 67\%$  of all the nights on Maunakea over the past five years the ground layer is easily separable from the free atmosphere layers based on wind speed and direction alone.

#### 3.2 Simulations

To further demonstrate the feasibility of temporal tomography in GLAO systems we have run simulations of a handful of illustrative cases. In each case we simulated an open loop GLAO system consisting of 1, 2, 3, or 5 natural guide stars. We used the University of Hawaii 88" telescope (UH88") aperture, 2.2 m in diameter with a central obscuration 0.891 m in diameter. Wavefront sensors were Shack-Hartmann-like with 8 × 8 subapertures and a frame rate of 200 Hz, in line with the 'imaka GLAO demonstrator on the UH88" telescope. <sup>10</sup> Slopes were calculated as a direct average of the gradient of the phase screen in a subaperture, with no additional noise. Guide stars were spaced equally along a circle of diameter 15' except in the 1 guide star case, which was on-axis.

The atmosphere was a two-layer atmosphere, one layer at a height of 0 m (the ground layer) and one at 2 km (the free atmosphere). Phase screens are evolved following the approach of Assémat et al (2006).<sup>11</sup> Finally, for each case we also simulated a second one-layer atmosphere that was composed of an identical ground-layer with no free atmosphere.

The simulated cases consisted of three night types: 1) a ground layer dominant night, where the ground layer contributes  $\frac{3}{4}$  of the total phase variance, 2) an equal strength night, where the two layers contribute equally, and 3) free atmosphere dominant night, where the free atmosphere contributes  $\frac{3}{4}$  of the total phase variance. For each of these night types we also varied the free atmosphere wind speed, from 1 to 3 times (in half steps) faster than ground layer wind speed of 6.5 m/s. In all cases the ground layer moves to the North, while the free atmosphere moves to the East.

For each simulated case open loop slopes were recorded for 8192 steps. At each step we did three different reconstructions using the Southwell geometry.  $^{12}$  The first is the standard estimate of the ground layer, which takes the reconstructed wavefront from each available guide star and averages them together. The second is the temporal tomography version. In this case we applied a notch reject recursive filter to the slopes' complex Fourier modes, the bandwidth was a fixed 15 Hz and the central frequency for each mode was set by  $f_t$  given by Eq. 1, plugging in the known free atmosphere wind vector. After filtering the Fourier modes for each guide star we applied the inverse DFT, reconstructed the wavefronts, and averaged them together. The third case is from the simulations where only the ground layer is present. Because they had no free atmosphere included it represented the best possible reconstruction of the ground layer. The residual wavefront from the difference between one of our estimates and this idealized measure is the amount of free atmosphere turbulence included in that estimate. We calculated the variance of the residual wavefronts for both estimates at every time step in each simulation, and then took the mean of each series of 8192 variances. These mean variances are plotted in Fig. 2, the smaller these variances are the better, with a value of 0 meaning the system matched the perfect case exactly.

In general we see that as the number of guide stars increases, the overall benefit of temporal tomography decreases, this is expected as you are averaging over more realizations of the free atmosphere turbulence. On nights when the free atmosphere is dominant, temporal tomography helps 2 and 3 guide star systems substantially, offering performance that is comparable to having 5 guide stars in the standard approach. On nights where the layers are of equal strength, 2 and 3 guide star systems benefit—though not as strongly as when the free atmosphere dominates. For ground layer dominant nights and equal strength nights with 5 guide star systems the filtered slopes actually produce a worse estimate of the ground layer than doing nothing at all. This is because the power of atmospheric layers is only strongest at  $f_t$ , they still contribute power at other temporal frequencies. Therefore, the deep notch reject filter used here is also filtering out the ground layer's contribution at  $f_t$ . As conditions shift towards ground layer dominated conditions the relative contributions to the total power at  $f_t$  shift as well requiring less aggressive filtering to remove the free atmosphere contribution. Finally, we see that the faster the free atmosphere wind speed is the more effective temporal tomography is, which is simply a statement that the larger the difference in  $f_t$  values between two layers, the easier it is to treat them separately. We find these results highly encouraging, especially given the clear avenues we have for improving the performance of temporal tomography in all conditions.

# 4. CONCLUSION

We have introduced the basic concept of a GLAO system that leverages temporal tomography for improved reconstructions of the ground layer turbulence. Using meteorological data dating back to January 1st, 2018 we demonstrate that conditions on Maunakea are typically favorable for the use of temporal tomography. Finally, we used open loop AO simulations to demonstrate that even a naive implementation of the temporal tomography approach yields improved estimates of the ground layer turbulence, though this does depend on the atmospheric conditions. In the future we will work on optimizing the filter design, which is expected to further improve our reconstruction of the ground layer, as well as to expand the range of conditions in which such an approach is helpful. Additionally, we plan to perform on-sky tests using the 'imaka GLAO demonstrator on the UH 88".

### ACKNOWLEDGMENTS

The authors would like to acknowledge the funding support of the National Science Foundation AST-1910552.

#### REFERENCES

- [1] Wilson, R. W., "SLODAR: measuring optical turbulence altitude with a Shack-Hartmann wavefront sensor," MNRAS 337, 103–108 (Nov. 2002).
- [2] Cortés, A., Neichel, B., Guesalaga, A., Osborn, J., Rigaut, F., and Guzman, D., "Atmospheric turbulence profiling using multiple laser star wavefront sensors," MNRAS 427, 2089–2099 (Dec. 2012).
- [3] Sivo, G., Turchi, A., Masciadri, E., Guesalaga, A., and Neichel, B., "Towards an automatic wind speed and direction profiler for Wide Field adaptive optics systems," MNRAS 476, 999–1009 (May 2018).
- [4] Poyneer, L., van Dam, M., and Véran, J.-P., "Experimental verification of the frozen flow atmospheric turbulence assumption with use of astronomical adaptive optics telemetry," *Journal of the Optical Society of America A* **26**, 833 (Mar. 2009).
- [5] Cortés, A., Rudy, A., Neichel, B., Poyneer, L., Ammons, S. M., and Guesalaga, A., "Analysis of the frozen flow assumption using GeMS telemetry data," in [Proceedings of the Third AO4ELT Conference], Esposito, S. and Fini, L., eds., 81 (Dec. 2013).
- [6] Roddier, F., Northcott, M. J., Graves, J. E., McKenna, D. L., and Roddier, D., "One-dimensional spectra of turbulence-induced Zernike aberrations: time-delay and isoplanicity error in partial adaptive compensation," *Journal of the Optical Society of America A* 10, 957–965 (May 1993).
- [7] Poyneer, L. A. and Véran, J.-P., "Optimal modal Fourier-transform wavefront control," *Journal of the Optical Society of America A* 22, 1515–1526 (Aug. 2005).
- [8] Poyneer, L. A., Macintosh, B. A., and Véran, J.-P., "Fourier transform wavefront control with adaptive prediction of the atmosphere," *Journal of the Optical Society of America A* 24, 2645 (Jan. 2007).
- [9] Yamartino, R. J., "A comparison of several "single-pass" estimators of the standard deviation of wind direction," *Journal of Applied Meteorology and Climatology* **23**(9), 1362 1366 (1984).
- [10] Chun, M. R., Lai, O., Toomey, D., Lu, J. R., Service, M., Baranec, C., Thibault, S., Brousseau, D., Hayano, Y., Oya, S., Santi, S., Kingery, C., Loss, K., Gardiner, J., and Steele, B., "Imaka: a ground-layer adaptive optics system on Maunakea," in [Adaptive Optics Systems V], Marchetti, E., Close, L. M., and Véran, J.-P., eds., Society of Photo-Optical Instrumentation Engineers (SPIE) Conference Series 9909, 990902 (July 2016).
- [11] Assémat, F., Wilson, R., and Gendron, E., "Method for simulating infinitely long and non stationary phase screens with optimized memory storage," *Optics Express* 14, 988–999 (Feb. 2006).
- [12] Southwell, W. H., "Wave-front estimation from wave-front slope measurements," *Journal of the Optical Society of America* (1917-1983) 7, 998 (Aug. 1980).